Radiation Induced Solid State Polymerization of Derivatives of Methacrylic Acid. V. An Electron Spin Resonance Study of Radical–Molecule and Radical–Radical Reactions in Barium Methacrylate Dihydrate

M. J. Bowden and J. H. O'Donnell

Chemistry Department, University of Queensland, Brisbane, Australia.
Received May 21, 1968

ABSTRACT: The electron spin resonance spectrum of γ-irradiated barium methacrylate dihydrate at −196° corresponded to approximately 90% of the initiating radical $(CH_3)_2\dot{C}COO^-$ and 10% of the propagating radical $RCH_2\dot{C}(CH_3)COO^-$. The total radical yield at −196° increased linearly with radiation dose up to 1 Mrad, corresponding to G(radicals) = 4.7 ± 0.5, but deviated increasingly from linearity at higher doses. On warming above −100°, the spectrum changed to that of the propagating radical, without any change in the total radical concentration. This radical transformation was temperature and time dependent and was attributed to the reaction $(CH_3)_2\dot{C}COO^- + CH_2{=}C(CH_3)COO^- \rightarrow (CH_3)_2C(COO^-)CH_2\dot{C}(CH_3)COO^-$. The kinetics of the reaction were studied in the temperature range −90 to −60°. It proceeded rapidly at first, followed by a much slower reaction. Both stages showed first-order dependence on the concentration of the initiating radical and gave Arrhenius activation energies of 2.6 ± 0.1 and 4.3 ± 0.4 kcal, respectively. At 50° polymerization to long-chain polymer occurred. This was accompanied by a marked decrease in radical concentration. The kinetics of the decrease were studied and the decay was attributed to the mutual interaction of short-chain, propagating radicals.

There have been numerous studies by electron spin resonance (esr) of the reactions of radicals produced in solids by γ irradiation. However, these have almost all been concerned with decreases in radical concentration on warming,[1-3] including rapid reactions at phase changes.[4-6] Such decreases occur by mutual interaction of pairs of radicals and are therefore diffusion-controlled reactions. Hence little information can be obtained about chemical parameters.

The production of a high concentration of radical I—$(CH_3)_2\dot{C}COO^-$—in γ-irradiated barium methacrylate dihydrate at −196° has been established.[7] It has also been shown that the propagation reaction involving addition of monomer molecules proceeds on warming. Long-chain polymer is formed at +50°,[8] but addition of the first monomer unit occurs at temperatures as low as −100°. This step, corresponding to reaction 1,

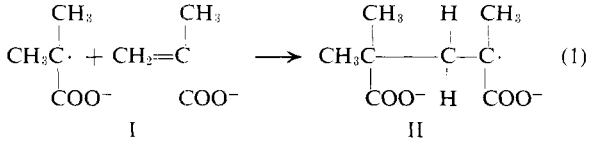

can be followed by observation of the changes in the esr spectrum. The spectrum of the initiating radical (I) consists of seven lines with a binomial intensity distribution and a hyperfine splitting (hfs) of 23 G, whereas the spectrum of the dimeric propagating radical (II) at −80° contains nine lines with an increasing intensity distribution and hfs of 11.5 G.[9]

Such a radical–molecule reaction should not be controlled by the diffusion parameters which are paramount in radical–radical reactions. A radical formed in the solid monomer would be surrounded by a shell of monomer molecules, and even assuming that the reaction is topochemically controlled,[8] diffusion would only have to occur over a distance of a few ångströms.[10]

The first part of this paper describes a detailed investigation of reaction 1 at various temperatures in the range −90 to −60°. Polymerization to long-chain polymer, *i.e.*, repeated addition of monomer molecules to the propagating radicals, occurs at temperatures greater than 25°. Termination of these long-chain propagating radicals by mutual interaction should be negligible in the solid state and the radical concentration would be expected to remain constant. This has been observed in the γ-radiation-induced polymerization of octadecyl methacrylate.[4] In barium methacrylate dihydrate a marked decrease in the concentration of propagating radicals was observed during polymerization at temperatures from 40 to 55°. Therefore kinetic studies were made of this decrease at 40, 50, and 55° and are reported in the second part of the paper.

Experimental Section

Barium methacrylate was prepared and the dihydrate recrystallized as described previously.[7] Powder samples were sealed under vacuum in Spectrosil tubes and irradiated with γ-rays at −196°.

(1) W. E. Griffiths and L. H. Sutcliffe, *Trans. Faraday Soc.*, **62**, 2837 (1966).
(2) S. E. Bresler and E. N. Kazbekov, *Fortschr. Hochpolym. Forsch.*, **3**, 688 (1964).
(3) H. Yoshida and B. Ranby, *J. Polym. Sci., Part B*, **2**, 1155 (1964).
(4) M. J. Bowden and J. H. O'Donnell, *ibid.*, in press.
(5) H. Szwarc, *J. Chim. Phys.*, **63**, 137 (1966).
(6) S. Nara, H. Kashiwabara, and J. Sohma, *J. Polym. Sci., Part A-2*, **5**, 929 (1967).
(7) J. H. O'Donnell, B. McGarvey, and H. Morawetz, *J. Amer. Chem. Soc.*, **86**, 2322 (1964).
(8) J. B. Lando and H. Morawetz, *J. Polym. Sci., Part C*, **4**, 789 (1964).
(9) M. J. Bowden and J. H. O'Donnell, *J. Phys. Chem.*, **72**, 1577 (1968).
(10) F. L. Hirshfeld and G. M. J. Schmidt, *J. Polym. Sci., Part A-1*, **2**, 2181 (1964).

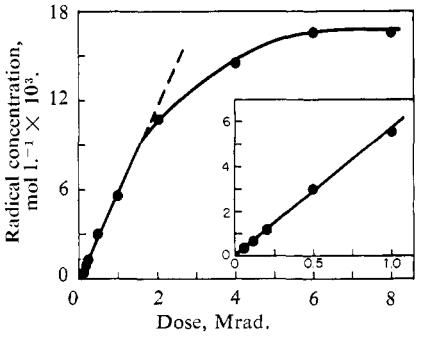

Figure 1. Radical yield at −196°.

Esr measurements were made with a Varian V4502 instrument using a liquid nitrogen dewar and variable temperature and dual sample cavities. Actual sample temperatures were obtained by calibration with a standardized thermocouple. Kinetic runs in the range −90 to −60° were carried out in the esr cavity, where temperature control throughout a kinetic run as ±0.5°. For the studies at 40–55° samples were kept in a constant-temperature bath between measurements.

Relative radical concentrations were obtained by double integration of the recorded first differential spectra using a computer. Absolute values were obtained by comparison with standard samples of α,α-diphenylpicrylhydrazyl (DPPH)–KCl mixtures.[11] The DPPH (Light and Co.) was recrystallized four times from carbon disulfide and dried in a vacuum oven for 10 hr at 70°. Standard samples were prepared by grinding and mixing weighed amounts of DPPH and KCl in a vibratory ball mill, or in an agate mortar. They were then sealed under a vacuum of 10^{-6} torr.

The proportions of initiating and propagating radicals in each sample were derived by three methods: (1) by measuring the decrease in height of the outermost lines due to radical I, (2) by measuring the increase in height of the intermediate lines due to radical II, and (3) by comparing computed spectra containing various proportions of I and II with the observed spectra. The computed spectra were calculated using the C.S.I.R.O. CDC 3600 computer and drawn on a Calcomp plotter.[9] Methods 1 and 2 could be used since there was no significant change in line width, or overlap of the two spectra at these positions. Method 3 is effectively an average of methods 1 and 2, taken over the whole spectrum, and is therefore the most satisfactory technique. The error resulting from using the computed spectra to determine the relative radical concentrations was estimated to be about ±3%.

Results and Discussion

Radical Yield at −196°. The total radical yield at −196° increased linearly with γ-radiation dose up to 1 Mrad as shown in Figure 1. The radiation chemical yield (G) was calculated from the slope to be 4.7 ± 0.05 radicals/100 eV. This is an abnormally high value for the production of trapped radicals in an organic solid and is one of the features of barium methacrylate dihydrate which makes it attractive for esr studies. On energetic grounds G(scission) of about 10 would be expected. However, in rigid media radical–radical recombination occurs very readily—the Franck Rabinowitch cage effect—thus accounting for the low G(trapped radical) values usually observed.[12-14] At

(11) K. H. Bar-Eli and K. Weiss, *J. Phys. Chem.*, **70**, 1677 (1966).

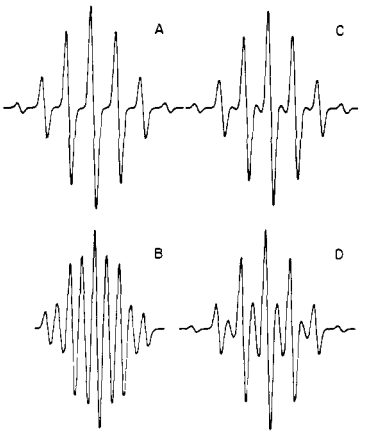

Figure 2. Esr spectra of (A) pure initiating radical ($R_1\cdot$), (B) pure propagating radical ($R_2\cdot$), (C) a mixture of 10% $R_2\cdot$ and 90% $R_1\cdot$, (D) a mixture of 50% $R_2\cdot$ and 50% $R_1\cdot$. These spectra apply to the temperature range −196 to −60° and for the short-chain propagating radical.[9]

higher radiation doses the plot of radical concentration *vs.* dose deviated increasingly from linearity. At high doses (>6 Mrad) it approached a saturation yield of radicals of about 1.7×10^{-2} M (10^{19} spins/cc or a mole fraction of 4.5×10^{-3}). This deviation from linearity is to be expected, particularly if the radicals are formed in spurs. Overlapping of the spurs at high doses then accounts for the deviation from linearity.[15]

After all doses the main radical species was the initiating radical I but some propagating radicals (II) were always present. We have previously shown[9] that the esr spectrum of the propagating radical depends on three factors: (1) the environment of the radical, (2) the temperature, and (3) the degree of polymerization, and that at −196° the propagating radical would most probably be a dimer radical in a monomer matrix. Therefore, the spectrum of the propagating radical in irradiated monomer at −196° was calculated assuming a 58–62° conformation of the β-methylene C–H bonds in the radical. Comparison of experimentally observed spectra with computed spectra synthesized from differing proportions of the initiating and propagating radicals showed that the two radicals were present in the approximate proportions of 90% I and 10% II after all radiation doses. The calculated esr spectra of the initiating radical (I), the propagating radical (II), and mixtures of I and II containing 10 and 50% of II are shown in Figure 2. The small amount of propagating radical must arise during irradiation since no further conversion of radical I to radical II was observed at −196°. It may be attributed to reaction 1 occurring as a result of the excitation energy of some of the initiating radicals overcoming the activation energy barrier, *i.e.*, "hot" radical reactions,

(12) I. Norman and G. Porter, *Proc. Roy. Soc.* (London), **A230**, 399 (1955).
(13) R. V. Bensasson, A. Bernas, M. Bodard, and R. Marx in the Proceedings of the Radiation Chemistry Symposium, Tihany, 1962, J. Dabo, Ed., Hungarian Acadamy of Sciences, Budapest, 1964.
(14) A. Chapiro and Y. Amagi, *J. Chim. Phys.*, **59**, 537 (1962).
(15) A. T. Bullock, W. E. Griffiths, and L. H. Sutcliffe, *Trans. Faraday Soc.*, **63**, 1846 (1967).

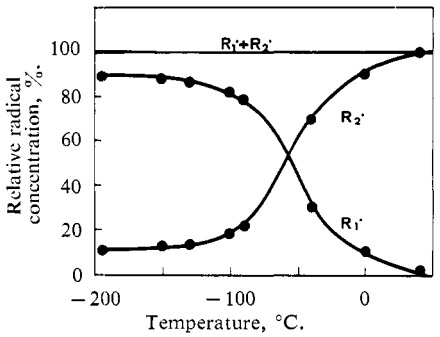

Figure 3. Temperature dependence of the radical concentrations during warming.

or to the formation of some of the radicals in defects which favor particularly high reactivity.

Radical Transformation above −100°. Temperature Dependence. When irradiated samples were warmed above −100° the seven-line spectrum of the initiating radical disappeared and the nine-line spectrum of the propagating radical appeared. There was no change in the total radical concentration. Figure 3 shows the effect of temperature on the proportions of the two radicals. In these measurements the sample was warmed to the required temperature, allowed to attain thermal equilibrium (approximately 2–7 min), then cooled back to −150° and the spectrum recorded. Since the total radical concentration remained constant and the observed spectrum could always be quantitatively accounted for by a mixture of radicals I and II, we conclude that reaction 1 proceeded on warming above −100°.

Time Dependence. The transformation was also time dependent at any temperature. The disappearance of radical I and the appearance of radical II were followed as a function of time at selected temperatures in the range −90 to −60°. Results obtained by measuring (1) the disappearance of the outer lines of the spectrum of radical I, or (2) the increase in intensity of the intermediate lines of the spectrum of radical II, or (3) comparing computed spectra containing I and II in various proportions with the observed spectra containing I and II in various proportions with the observed spectra gave similar kinetic curves. The computed spectra of radicals I and II are the same from −196 to −50° and are as shown in Figure 2.

The change in the concentration of the initiating radical with time at a series of constant temperatures is shown in Figure 4. At each temperature the rate of disappearance of radical I was initially very high, but then decreased to a relatively low value. At higher temperatures this decrease occurred after greater proportions of the initiating radical concentration had reacted. If the reaction followed normal kinetics, then

$$\frac{-\mathrm{d}[\mathrm{R}_1\cdot]}{\mathrm{d}t} = k_2[\mathrm{R}_1\cdot][\mathrm{M}]$$

where $[\mathrm{R}_1\cdot]$ is the concentration of the initiating radical and [M] is the concentration of monomer. Assuming the monomer concentration to remain unchanged by the first addition

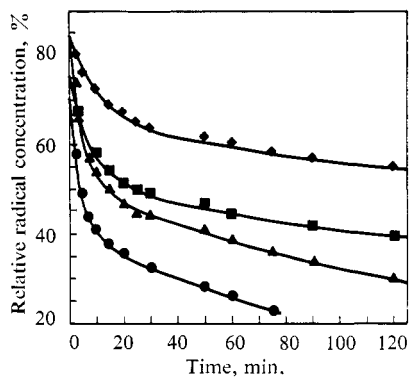

Figure 4. Time dependence of initiating radical concentration ($R_1\cdot$] at constant temperatures: ●, −60°; ▲, −70°; ■, −80°; ◆, −90°.

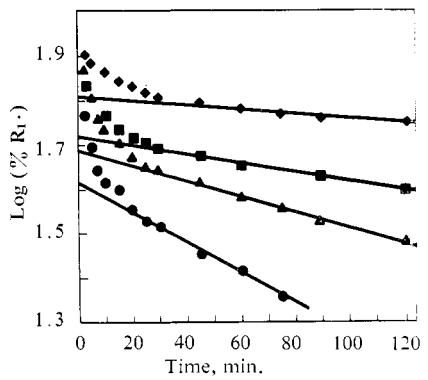

Figure 5. Kinetic plots for reaction of initiating radical ($R_1\cdot$): ●, −60°; ▲, −70°; ■, −80°; ◆, −90°.

$$\frac{-\mathrm{d}[\mathrm{R}_1\cdot]}{\mathrm{d}t} = k_1[\mathrm{R}_1\cdot]$$

where $k_1 = k_2[\mathrm{M}]$; one would expect first-order kinetics with respect to the initiating radical concentration. Plots of log $[\mathrm{R}_1\cdot]$ against time are shown in Figure 5. Initially the plots are curved, but after a certain time they obey a linear relationship.

The experimental results can be explained by considering the over-all reaction to be due to two parallel, first-order reactions, both producing the dimeric propagating radical $\mathrm{R}_2\cdot$. Consideration of the reaction scheme

$$\mathrm{R}_1{}^*\cdot + \mathrm{M} \xrightarrow{k_a} \mathrm{R}_2\cdot \qquad (2)$$

$$\mathrm{R}_1\cdot + \mathrm{M} \xrightarrow{k_b} \mathrm{R}_2\cdot \qquad (3)$$

leads to the rate equations

$$-\mathrm{d}[\mathrm{R}_1{}^*\cdot]/\mathrm{d}t = k_a{}^1[\mathrm{R}_1{}^*\cdot]$$

and

$$-\mathrm{d}[\mathrm{R}_1\cdot]/\mathrm{d}t = k_b{}^1[\mathrm{R}_1\cdot]$$

which integrate to

$$[\mathrm{R}_1{}^*\cdot] = [\mathrm{R}_1{}^*\cdot]_0 e^{-k_a{}^1 t}$$

and

$$[\mathrm{R}_1\cdot] = [\mathrm{R}_1\cdot]_0 e^{-k_b{}^1 t}$$

Since the reaction is followed by measuring $[\mathrm{R}_1{}^*\cdot +$

TABLE I
KINETIC PARAMETERS FOR THE REACTION $R_1\cdot + M \rightarrow R_2\cdot$

	Temperature, °C			
	−60	−70	−80	−90
		Fast Reaction		
k_1, sec^{-1}	$3.77 \pm 0.07 \times 10^{-3}$	$2.62 \pm 0.16 \times 10^{-3}$	$1.98 \pm 0.05 \times 10^{-3}$	$1.38 \pm 0.03 \times 10^{-3}$
k_2, l. mol^{-1} sec^{-1}	$10.20 \pm 0.19 \times 10^{-4}$	$7.10 \pm 0.43 \times 10^{-4}$	$5.36 \pm 0.13 \times 10^{-4}$	$3.74 \pm 0.10 \times 10^{-4}$
E_a, kcal mol^{-1}		2.6 ± 0.1		
A, l. mol^{-1} sec^{-1}		0.4 ± 0.1		
		Slow Reaction		
k, sec^{-1}	$1.33 \pm 0.07 \times 10^{-4}$	$0.73 \pm 0.02 \times 10^{-4}$	$0.39 \pm 0.03 \times 10^{-4}$	$0.25 \pm 0.02 \times 10^{-4}$
k_2, l. mol^{-1} sec^{-1}	$3.60 \pm 0.19 \times 10^{-5}$	$1.98 \pm 0.06 \times 10^{-5}$	$1.06 \pm 0.10 \times 10^{-5}$	$0.15 \pm 0.06 \times 10^{-5}$
E_a, kcal mol^{-1}		4.3 ± 0.4		
A, l. mol^{-1} sec^{-1}		0.9 ± 0.1		

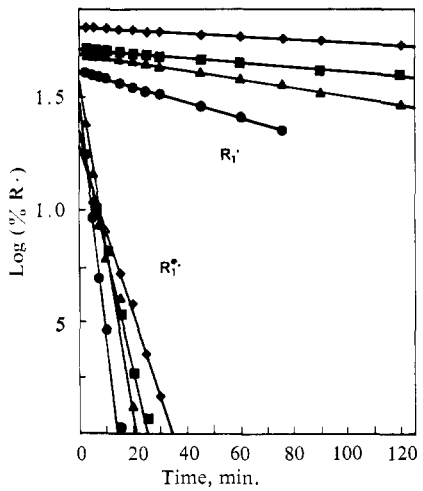

Figure 6. Kinetic analysis of Figure 4 in terms of two parallel first-order reactions: ●, −60°; ▲, −70°; ■, −80°; ◆, −90°.

$R_1\cdot]$, the sum of the concentrations of the two reactants, then the above equations predict that

$$\log [R_1^*\cdot + R_1\cdot] = \log \{[R_1^*\cdot]_0 e^{-k_a^1 t} + [R_1\cdot]_0 e^{-k_b^1 t}\}$$

Further, provided $k_a \neq k_b$, a plot of log $[R_1^*\cdot + R_1\cdot]$ *vs.* time should be curved (*cf.*, Figure 5). If $k_a \gg k_b$, then the more reactive component $R_1^*\cdot$ would be expected to disappear after a certain interval, when the expression for log $[R_1^* + R_1\cdot]$ would become

$$\log [R_1^*\cdot + R_1\cdot] = \log [R\cdot_1] = \log [R_1\cdot]_0 - k_b^1 t$$

i.e., the curve should become linear, as is observed in Figure 5. From the slope and intercept of this line, $[R_1\cdot]_0$ and k_b^1 may be determined and $[R_1\cdot]$ found at any time. With this information $[R_1^*\cdot]$ may be calculated, and hence the rate constant of the first reaction may be determined from the slope of log $[R_1^*\cdot]$ *vs.* time.[16] Figure 6 shows the plots of log $[R_1^*\cdot]$ and log $[R_1\cdot]$ *vs.* time.

We suggest that $R_1\cdot$ and $R_1^*\cdot$ represent the same chemical radical species—initiating radicals (I)—trapped in two basically different environments. These may be (a) oriented in the crystal lattice, and (b) not oriented. It has been well established by many workers that some radicals produced in single crystals of organic compounds by γ irradiation may be oriented in the lattice, whereas others are not. Moreover, the oriented radicals are usually less reactive and remain after careful warming, when the other radicals react. Presumably the oriented radical is in a relatively nondefect site and the unoriented radical must be in a defect site, which may be produced during crystal growth or by the irradiation. Unfortunately, the isotropic nature of the initiating radical spectrum prevents distinction between these two cases by single crystal studies. Although two types of initiating radical (I) with markedly different rates of reaction with monomer can be distinguished, this is an oversimplification and there must be a range of trapping sites with a spectrum of energies for detrapping and subsequent reaction.[17]

Observation of the esr spectrum with time has been shown to be a method of studying the kinetics of a radical–molecule reaction (reaction 1) in the solid state at low temperatures. The slopes of kinetic plots of the changes in radical concentrations give quantitative measures of the rates. If first-order kinetics are considered to be applicable, rate constants can be derived without the actual radical or monomer concentrations being required. These are listed for the fast and slow reactions in Table I. The temperature dependence of the rates indicates Arrhenius activation energies for the fast and slow reactions of 2.6 ± 0.1 and 4.3 ± 0.4 kcal, respectively.

Second-order rate constants can be calculated from these first-order rate constants, if a value can be assigned to the monomer concentration, since $k_1 = k_2$[M]. We have taken this to be the bulk concentration of the monomer in the solid. The results (Table I) indicate that the rate constant in the solid at −75° is about 10^{-4} of the hypothetical value for the propagation step in the polymerization of methyl methacrylate in the liquid phase at that temperature (calculated from A and E_a values for the above-ambient reaction[18]).

Radical Decay at 40–55°. When irradiated samples were warmed to 40–55° and maintained at constant temperature the total radical concentrations decreased with time to apparent limiting concentrations of about 30–50% of the initial values. The decreases in radical concentration with time at 40, 50 and 55° are shown in Figure 7 (curves A, B and C). Measurements were

(16) A. A. Frost and R. G. Pearson in "Kinetics and Mechanism," 2nd ed, John Wiley & Sons, Inc., New York, N. Y., 1961, p 162.

(17) J. M. Flournoy, L. H. Baum, and S. Siegel, *J. Chem. Phys.*, **36**, 2229 (1962).

(18) A. M. North in "Kinetics of Free Radical Polymerization," Pergamon Press Ltd., London, 1966, p 58.

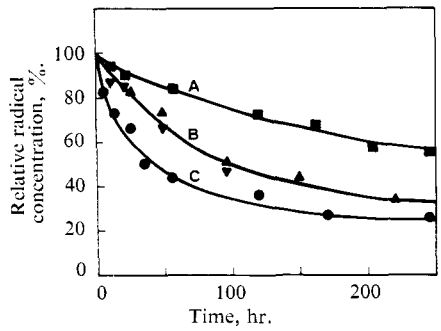

Figure 7. Radical decay at 40–50°: ■, 40° (A); ▲ and ▼, 50° (B); ●, 55° (C).

also made at times considerably in excess of the 240 hr shown, but no further decreases in radical concentrations were observed. It seems quite definite that the radical concentrations reach limiting values. The rate of decay was greater and the limiting concentration lower at higher temperatures. Limiting values of 48, 30 and 27% were obtained at 40, 50 and 55°, respectively.

The kinetics of the radical decay were examined in detail at all three temperatures. The analysis is discussed for 50°, similar results being obtained for 40 and 55°. We will consider several possible methods of analyzing the kinetic data and the mechanistic feasibility in each case.

1. When irradiated barium methacrylate dihydrate is warmed to 40–55° all the radicals are methacrylate propagating radicals, $RCH_2\dot{C}(CH_3)COO^-$, and the decrease in total radical concentration might be expected to follow first- or second-order kinetics. The appropriate plots are shown in Figure 8 (curves D and E). There is an appreciable deviation from first-order, but good agreement with second-order kinetics up to about 200 hr. However, beyond this time there is no significant further decrease in radical concentration.

2. An assumption that can be made is that there are two types of dimeric propagating radicals present from the beginning: (a) those capable of further propagation, and (b) those unable to propagate any further—perhaps due to the nature of their trapping site in the lattice. There are then two possibilities: either (1) only type a can terminate, or (2) only type b can terminate. For either case, the concentration of the radicals which can terminate may be found at any time by subtracting the limiting concentration from the total concentration. The time dependence of this concentration was then tested for first-order and second-order decay (curves F and G in Figure 8). There is good agreement with first-order, but no correlation with second-order kinetics. However, there is no direct evidence to support the concept of two different radical populations in the temperature range 40–55°.

3. A further possibility can also be considered. The probability of termination may decrease as the length of the chain increases. Radicals which are finally trapped must then be long-chain radicals. This is supported by the difference between the initial and final esr spectra, which we have attributed to the increase in chain length.[9] The restricted mobility of the long chains and the statistical improbability of their

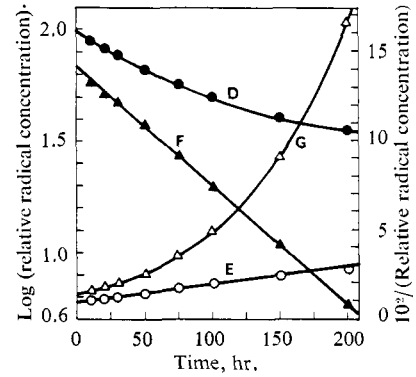

Figure 8. Kinetic plots for radical decay at 50°: D, first order; E, second order plots for total radical concentration; F, first order; G, second order plots for concentration of radicals which can terminate.

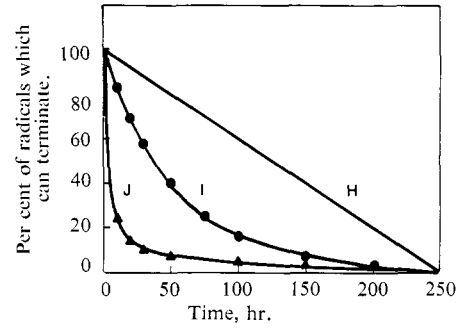

Figure 9. Functions for time dependence of concentration of radicals which can terminate.

radical ends meeting would also suggest this. Therefore, initially all radicals will have the possibilities of terminating or propagating, and finally they will have zero probability of doing either. An arbitrary function for the relative concentration of radicals able to terminate, *vs.* time, can be drawn, and three cases are shown in Figure 9. These are (1) linear (H), (2) logarithmic (I), and (3) hyperbolic (J).

For each case the concentration of radicals which (a) can terminate and (b) cannot terminate can then be obtained as functions of time, and are shown in Figure 10. The logarithmic and hyperbolic functions lead to impossible curves for concentrations of radicals which cannot terminate, therefore functions 2 and 3 must be rejected. We have considered one further case (4) in which the concentration of radicals which cannot terminate follows a curve of similar shape to that frequently obtained for the conversion in post-irradiation polymerization (curve P in Figure 10).

The time dependence of the concentration of radicals which can terminate ($R_t\cdot$) fits first-order kinetics for both cases 1 and 4, as shown in Figure 11. At any time, the radicals which are able to terminate can participate in either of two reactions

$$R\cdot + M \longrightarrow R_p\cdot$$

$$\text{rate} = k_2[M][R\cdot] \quad (4)$$

$$R\cdot + R\cdot \longrightarrow RR \text{ or } RH + R'C{=}CH_2$$

$$\text{rate} = k_2'[R\cdot]^2 \quad (5)$$

Both reactions are bimolecular, but it would be expected that reaction 4 would be first order because the

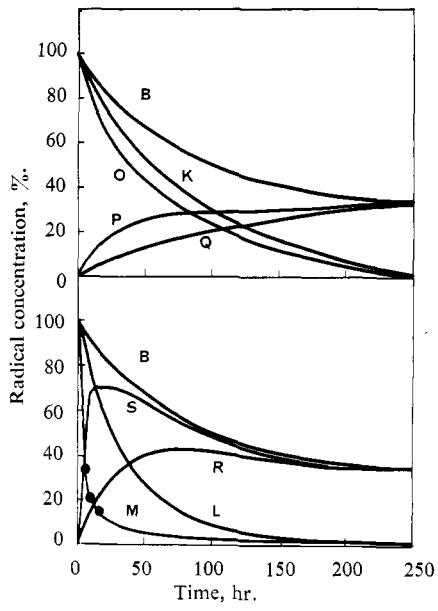

Figure 10. Calculated time dependence of radical concentrations at 50°. B is the experimental total radical concentration; ●, experimental concentrations of short-chain radicals from esr spectra: i, radials which can terminate; ii, radicals which cannot terminate.

function	i	ii
linear (H)	K	Q
logarithmic (I)	L	R
hyperbolic (J)	M	S
case 4 in text	O	P

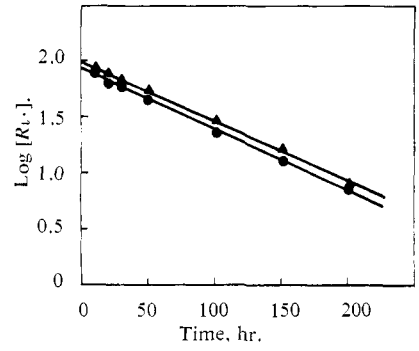

Figure 11. First-order kinetic plots for radical decay at 50°: ▲, case 1; ●, case 4, in text.

monomer (M) concentration is effectively constant. Since the over-all reaction is first order when allowance is made for the limiting radical concentration, it therefore appears that reaction 5, the radical decay, must also be first order. From the kinetic plots in Figure 11 only a combined rate constant for the two reactions can be determined and the individual rate constants cannot be resolved.

Further information on the reactions can be obtained from the nature of the esr spectra. The shape changes with time, as shown in Figure 12, from increasing to alternating line intensities. This change is initially very rapid, and can be attributed, before appreciable conversion to polymer, to a change from short-chain to medium-chain propagating radicals. The relative

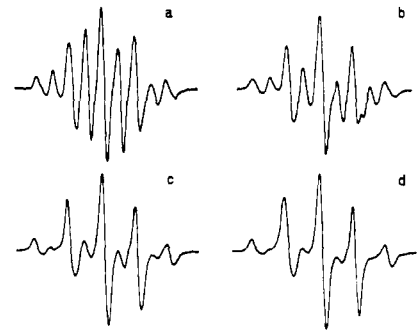

Figure 12. Esr spectra of propagating radical during polymerization at 50°: □ a, O hr; b, 5 hr; c, 96 hr; d, 180 hr.

proportions of short-chain and medium-chain radicals can be determined from the relative peak heights in the spectra and the decrease in short-chain radical concentration with time is shown in Figure 10. It is much more rapid than the decrease in the concentration of radicals which can terminate.

The picture which emerges is that of a rapid decrease in the concentration of short-chain radicals. Repeated addition of monomer molecules produces a progressively increasing average chain length. The rate of mutual termination decreases with increasing chain length and also as radicals in close proximity to one another, which are probably formed in spurs, combine.

The temperature dependence of the decrease in total radical concentration is probably best derived from first-order plots of type F in Figure 8, a value for the Arrhenius activation energy of 14 ± 4 kcal being obtained.

The possible effects of the water molecules on the reaction should not be disregarded. They comprise two out of every three molecules, or about 10% of the volume, in the crystal. First, they probably provide the hydrogen atoms which add to the double bond of the monomer to produce $R_1\cdot$. Second, as we have shown previously,[9] the radical end of the growing chain adopts an increasing twist away from the symmetrical conformation, which is probably due, in part, to plasticizer action by the water. The involvement of the water in the propagation reaction is under further investigation.

Conclusions

It has been shown that in barium methacrylate dihydrate the addition of the first monomer molecule to the initiating radical occurs at a much lower temperature than the subsequent repeated addition of monomer molecules to the propagating radical to form long-chain polymer. The rate of the first addition is temperature dependent with an Arrhenius activation energy suggesting possible chemical control. The reaction occurs with a fast and a slow stage indicating a variation in the energy of the trap for the initiating radical. A marked decrease in the radical concentration during polymerization to long-chain polymer at 50° has been observed, which can be explained by diffusion

and mutual interaction of short-chain radicals, especially if these occur in regions of high local radical concentration.

Acknowledgments. We wish to thank the Australian Institute of Nuclear Science and Engineering for supporting this project, the Australian Atomic Energy Commission, and particularly Mr. J. H. Bolton and Mr. B. M. O'Leary, for irradiation of samples, Professor L. E. Lyons for generously making the esr facilities available, and C.S.I.R.O. for providing a studentship for M. J. B.

Interactions in Solutions of Block and Statistical Copolymers of Styrene and Methyl Methacrylate

Lechoslaw A. Utracki[1a] and Robert Simha[1b]

Division of Polymer Science, Case Western Reserve University, Cleveland, Ohio 44106.
Received August 30, 1968

ABSTRACT: Intrinsic viscosities of block and statistical copolymers of styrene (S) and methyl methacrylate (M) are analyzed as a function of molecular weight and composition by means of relations recently applied to styrene–butadiene block polymers. The unperturbed dimensions of the block polymer are entirely determined by those of the individual blocks and the composition. In the statistical copolymers they depend on the placement probabilities of the various pairs along the chain, but the departure from the relation for block copolymers turns out to be small. The long-range interaction parameter can be expressed for both types of copolymers as a quadratic form in the composition. The polymer–polymer interaction factor varies with the polymerization conditions of the PMMA block, and a correlation with the heterotacticity index is shown to exist. In a series of samples with similar indices for heterotacticity the interaction parameter is independent of molecular weight, composition and number of blocks. Also, no systematic differences are observed between benzene and toluene at 25 and 30°.

The solution properties of block copolymers have been investigated for a number of years and the poly(methyl methacrylate) (PMMA)–polystyrene (PS) combination has been a preferred object of study. Frequently contradictory findings have been summarized at various occasions.[2-9]

We have recently measured the intrinsic viscosities and second virial coefficients of polystyrene–polybutadiene block copolymers[10] and given a description of the molecular weight and composition dependence. It is based on the concept of a θ temperature at which all long-range interactions vanish separately rather than on a mutual compensation which would make the θ temperature dependent on molecular weight and composition for a given solvent.[8,11,12] The purpose of this paper is to examine available experimental data on PS–PMMA di- and triblock copolymers on the basis of the relations developed previously.

Method of Analysis

Consider a block copolymer composed of a series of chemical species $i = 1, 2 \ldots n$. Let M_i be the molecular weight of species i, with a repeat unit of molecular weight M_{0i} (per one carbon bond of the backbone chain), unperturbed dimensions $\langle r_\theta^2 \rangle_i$, and short-range interaction parameter $A_i^2 = a_i^2/M_{0i} = \langle r_\theta^2 \rangle_i / M_i$. If x_i is the mole fraction and $B_i = \beta_i / M_{0i}^2$ the long-range interaction parameter, we write for the copolymer the averages[10] given in eq 1, where the subscript c refers to the copolymer. The second equation

$$M_{0c} = \sum_i x_i M_{0i}$$
$$a_c^2 = A_c^2 M_{0c} = \sum_i x_i a_i^2 \qquad (1)$$
$$\beta_c = B_c M_{0c}^2 = \sum_i \beta_{ii} x_i^2 + 2 \sum_{i<j} \beta_{ij} x_i x_j$$

expresses the Gaussian character of the chain at $T = \theta$, where all β_{ij} vanish. The third assumes that the fraction of i–j configurations characterized by an interaction parameter β_{ij} can be represented as a product of mole fractions. This, of course, is strictly valid only for a random distribution of segments, and should not be expected to hold if all the β's are sufficiently different from each other. In the styrene–butadiene system, eq 1 proved to be valid in solvents which are good for at least one of the components.[10] Equation 1 extends any two-parameter (A,B) relation developed for homopolymers to block copolymers by the introduction of additional quantities β_{ij}.

(1) (a) Research Center, Shawinigan Chemicals Ltd., Ste-Anne de Bellevue, Quebec. (b) To whom correspondence should be addressed.

(2) (a) G. M. Burnett, P. Meares, and C. Paton, *Trans. Faraday Soc.*, **58**, 737 (1962); (b) S. Krause, *J. Phys. Chem.*, **68**, 1948 (1964).

(3) J. R. Urwin and M. Stearne, *Makromol. Chem.*, **78**, 204 (1964).

(4) W. H. Stockmayer, L. D. Moore, Jr., M. Fixman, and B. N. Epstein, *J. Polym. Sci.*, **16**, 517 (1955).

(5) D. Froelich and H. Benoit, *Makromol. Chem.*, **92**, 224 (1966).

(6) A. Dondos, D. Froelich, P. Rempp, and H. Benoit, *J. Chim. Phys.*, **64**, 1012 (1967).

(7) D. Froelich, *ibid.*, **64**, 1311 (1967).

(8) H. Inagaki and Y. Miyamoto, *Makromol. Chem.*, **87**, 166 (1965).

(9) H. Inagaki, *ibid.*, **86**, 298 (1965).

(10) L. Utracki and R. Simha, *Amer. Chem. Soc., Div. Polym. Chem., Preprints*, **9**, 742 (1968); L. Utracki, R. Simha, and L. J. Fetters, *J. Polym. Sci., Part A-2*, in press. For the second virial coefficient of a statistical copolymer, a quadratic form in the composition (see eq 1) was given earlier by R. Simha and H. Branson, *J. Chem. Phys.*, **12**, 253 (1944).

(11) S. Schlick and M. Levy, *J. Phys. Chem.*, **64**, 883 (1960).

(12) T. Kotaka, H. Ohnuma, and Y. Murakami, *ibid.*, **70**, 4099 (1966).